2017; 21: 2970-2979

Effects of epoxyeicosatrienoic acids (EETs) on retinal macular degeneration in rat models

F. MEI^{1,2}, J.-G. WANG^{3,4}, Z.-J. CHEN¹, Z.-L. YUAN²

Abstract. - OBJECTIVE: Here we use a rat model to investigate the effects of epoxyeicosatrienoic acids (EETs) on retinal macular degeneration along with pathological and physiological mechanisms of the disease.

MATERIALS AND METHODS: Six choroidal neovascularization (CNV) rats were created with a 532 nm laser and received intravitreal injections of EETs in both eyes. On day 1, 3, 7 and 14 after photocoagulation, the thickness and area of CNV were measured with HE staining and choroidal flat mounts. COX-2 and VEGF levels in CNV were detected by immunohistochemistry method. Protein and mRNA expression were studied by Western blotting and RT-PCR.

RESULTS: 14 days after photocoagulation, CNV thickness and area were significantly reduced (p<0.01) in the treatment group compared with the control group. COX-2 and VEGF had high expression in vascular endothelial cells and stromal cells of CNV. Peak expression of COX-2 and VEGF was significantly higher (p<0.01) in the treatment group than in the control group. 7 days after photocoagulation, VEGF protein and mRNA expression were significantly lower (p<0.05) in the treatment group than in the control group, whereas COX-2 mRNA showed no significant difference (p>0.05). FFA found that CNV fluorescein leakage area was significantly reduced (p<0.05) in the treatment group than in the control group. 14 days after photocoagulation, neovascularization area was significantly smaller (p<0.05) in the treatment group than in the control group. Vitreous EETs levels in the treatment group were significantly higher than in the control group. Compared with the control group, the celecoxib treatment group had significantly increased vitreous EETs (p<0.05).

CONCLUSIONS: Intravitreal injection of celecoxib could suppress the thickness and area of laser-induced macular degeneration CNV. It also improved the vitreous EETs levels in CNV model rats. COX-2 expression was upregulated in the early generation of laser-induced CNV, which may play an important role in regulating expression of VEGF.

Key Words:

Macular degeneration, Choroidal neovascularization, Arachidonic acid, Vascular endothelial growth factor, Epoxyeicosatrienoic acids, EETs.

Introduction

Choroidal neovascularization (CNV) is one of the major pathological factors during the disease development of macular degeneration¹. CNV also occurs in other diseases such as age-related macular degeneration (AMD), vascular patterns change (AS), pathologic myopia and presumed ocular histoplasmosis disease syndrome (POHS)^{2,3}. Neovascularization originates from the choriocapillaris, breaks the bruch membrane and forms macular neo-vascular membrane. New vessels are fragile and easy to leak, so they are very likely to cause bleeding or oozing, which will damage the photoreceptor cells. Also, the proliferation of blood vessels is capable of forming a fibrous scar, resulting in irreversible damage to retinal function and even vision loss.

CNV generation is the result of an imbalance between localized angiogenic factors and angiogenesis inhibitors. Vascular endothelial growth factor (VEGF) is currently the strongest known angiogenic factor and is capable of stimulating endothelial cell proliferation and increasing endothelial permeability. Epoxyeicosatrienoic acids (EETs) are metabolites OD arachidonic acid (AA), which is processed by a large number of cytochrome P450s present in the liver⁴. Biological functions of EETs are very complicated. They can regulate migration and metastasis of tumor cells.

¹Department of Ophthalmology, Children's Hospital of Nanjing Medical University, Nanjing, Jiangsu, China

²Department of Ophthalmology, The First Affiliated Hospital of Nanjing Medical University, Nanjing, Jiangsu, China

³Department of Otolaryngology-Head and Neck Surgery, Nanjing Drum Tower Hospital Affiliated to Nanjing University Medical School, Nanjing, Jiangsu, China

⁴Research Institution of Otolaryngology, Nanjing, Jiangsu, China

Degradation of EETs by an epoxide degradation enzyme COX-2 will lead to the generation of CNV. In the past few years, EETs were found to function in CNV by regulating the expression of VEGF⁵⁻⁷. In this study, we investigate the function and biological effects of EETs on CNV in macular degeneration rat models, with an effort to provide a theoretical basis for the use of EETs to treat and prevent macular degeneration.

Materials and Methods

Experimental Animals and Reagents

Six male brown Norway (BN) rats of 8 to 12 weeks old with weights between 180-220 g were provided by Beijing Vital River Laboratory Animal (Co., Ltd., Beijing, China). The rats were kept at 24-26°C with a humidity of 60% and a 12 h/12 h light and darkness cycle. All animals had normal anterior segment and fundus examination results before the experiments. 20% fluorescein sodium injection (Wuzhou Pharmaceutical Co., Ltd., Guangdong, China); sodium pentobarbital (Sigma-Aldrich, St. Louis, MO, USA); rhodamine-labeled castor bean lectin (Vector, Torrance, CA, USA); 20% fluorescein sodium injection (Baiyunshan Mingxing Pharmaceutical Co., Ltd., Guangzhou China); heparin sodium injection (2 ml: 5000 u, Yangtze Pharmacol Co., Ltd., Taizhou, China); 4% paraformaldehyde in phosphate buffer PEA4og + o.IM-PBsl000nil, rabbit anti-human FVIIIR: Ag monoclonal antibody (Boster Biological Engineering Co., Ltd., Wuhan, China); AEC staining kit (Boster Biological Engineering Co., Ltd., Wuhan, China); FITC-D perfusion solutions: FITC-D20 mg (Dextran, fluorescein, Invitrogen, Carlsbad, CA, USA) + 5 ml Ringer's lactate + 0.5 g gelatin; 6% chloral hydrate solution; COX-2 rabbit anti-rat polyclonal antibody (Neo-Marker, Fremont, CA, USA); mouse anti-rat VEGF monoclonal antibody (Santa Cruz Biotechnology, Santa Cruz, CA, USA); normal goat serum (Zhongshan Golden Bridge Biotechnology, Co., Ltd., Beijing, China); SP secondary antibodies kit (Zhongshan Golden Bridge Biotechnology Co., Ltd., Beijing, China); AEC staining kit (Zhongshan Golden Bridge Biotechnology Co., Ltd., Beijing, China); glycerol vinyl alcohol-soluble mounting medium (GVA) (Zhongshan Golden Bridge Biotechnology Co., Ltd., Beijing, China); BCA method protein assay kit (Puli Lai Co., Ltd., Beijing, China); WB prestained protein (Fermentas Company, Vilnius, Lithuania); DNA marker DL2000 (Tiangen Co., Ltd., Beijing, China); Trizol (Invitrogen, Carlsbad, CA, USA); reverse transcription kit (Fermentas Co., Vilnius, Lithuania); primers (Biological Engineering Technology Services Co., Ltd., Shanghai, China).

Experimental Equipment

532 nm harmonic Nd: YAG laser (Quantel Medical, Cournon-d'Auvergne, France); ocular three-mirror lens (Ocular Inc., Bellevue, WA, USA); confocal laser angiography instrument (Heidelberg, Germany); electric oven (Yuejin Medical Instruments Factory, Shanghai, China); GTK-2002 automatic thermostat for slides spreading, baking and roasting (Ruifeng Equipment Company, Xian, China); Leica DM LB2 optical microscope (Leica, Wetzlar, Germany); stereo microscope (Zeiss, Oberkochen, Germany); digital camera IXUS100 (Canon IXUS700, Tokyo, Japan); laser scanning confocal microscope (Olympus LV100, Tokyo, Japan).

Production of Animal Models

6 BN rats received intravitreal injections of 10 ul drugs in both eyes. The right eyes were injected celecoxib (1 mg/ml); the left eyes were injected phosphate buffered saline (PBS) (0.01 M). Intraperitoneal injection of 1% pentobarbital sodium (50 mg/kg) was used to anesthetize the rats. Both eyes were then dilated with tropicamide eye drops and treated with medical sodium hyaluronate gel. The eyes were placed in front of 53.0 D corneal contact lens. A 532 nm laser through a slit lamp (Power: 80 mW, Laser spot diameter: 100 µm, Exposure time: 100 ms) was applied to create 8 to 10 photocoagulation points equidistantly at 1.5-2 PD from the vison disc. After the photocoagulation, the appearance of bubbles and/or mild bleeding (sometimes accompanied by light popping sound) meant breakage of bruch membrane, and these points were marked as the effective points8. All experimental operations followed Association for Research in Vision and Ophthalmology (ARVO) rules. Experimental animals in the study were SPF level laboratory animals, and all researchers have obtained permits to work with experimental animals.

Immediately after photocoagulation, rats were given intravitreal injection. Rat eyes were applied 1% tetracaine hydrochloride for topical anesthesia (while rats were still under general anesthesia at that time). Bulbar conjunctiva (close to and slightly above ear rats) were isolated under microscope to fully expose thee scleral wall. Number 27 needle was used to puncture a 0.5 mm incision in the sclera, and then a micro syringe was used

to inject 10 µl drugs (1 mg/ml celecoxib or 0.01 M PBS). The syringe entered through the incision and pointed directly to the vision disc to deliver the drugs to the vitreous. Successful deliveries of the drug into the vitreous and their positions were confirmed⁹.

Fluorescein Angiography

14 days after the laser photocoagulation, three eyes were randomly chosen from the intravitreal PBS group to perform fluorescein fundus angiography (FFA). Intraperitoneal injection of 1% sodium pentobarbital (50 mg/kg) was used for anesthesia. After dilation, 20% sodium fluorescein solution were injected intraperitoneally and the dosages were 0.5 ml/kg. FFA images were collected during 2-30 min period after injection. FFA images were grouped into early phase (< 2 min) and late phase (> 10 min). The generation of CNV was determined by whether late phase FFA images showed fluorescein leakage¹⁰.

Histopathological Observation

Anesthesia was done with intraperitoneal injection of 1% sodium pentobarbital (100 mg/ kg). After the disappearance of pain reflex of toes, abdominal walls were cut open below the sternum. Liver and other tissues were pushed aside to expose the diaphragm and apex beats were visible. The diaphragm was cut open away from the apex and then the chest wall was cut open to expose the heart. A syringe was inserted from the apex and pointed to the left ventricle and arrived at aorta. After vascular clamping, the right atrium was cut open and perfusion was conducted with about 400 ml 0.9% saline. Correct perfusions were determined by unexpanded lungs, no blood or water coming out of nose and mouth, and gradual whitening of liver and other tissues. Conjunctivas were cut along the limbus ring. Eyeballs were removed by cutting the extraocular muscles and optic nerves. Eyeballs were then fixed as follows; they were immersed in new style Bouin liquid for 24 h. Then, the connective tissues around the eyeballs were removed; cornea and lens were later removed by cutting along the limbus. The dehydration was conducted with 75%, 85% ethanol treatments for 3 h each, followed by 90%, 95%, 95%, 100%, 100% ethanol treatments for 2 h each. Routine HE staining was then performed.

CNV Thickness Measurement

All slices containing CNV were imaged with a CCD camera attached to an optical microscope.

The images were saved to a computer and numbered sequentially. Image-proplus 6.0 professional image processing software was used to measure CNV thickness (the vertical distance from the normal RPED layer to the highest point of the newly formed tissue). Included CNV should have good continuity and intact tissue. For the same CNV, the maximum thickness measurement among successive sections were chosen. For a certain time point, CNV thickness was recorded as the average thickness of at least 7 to 10 different CNV measurements^{9,11}. Experimental data were then evaluated by two professionals using independent double-blind assessment. SPSS12.0 software (SPSS Inc., Chicago, IL, USA) was used to perform independent samples t-tests.

RPE-Choroid-Sclera Flat Mounts

14 days after laser photocoagulation, rats were treated with excess anesthesia followed by cardiac perfusion with 400 ml of saline and 400 ml with 14% paraformaldehyde. The eyeballs were separated and fixed in 4% paraformaldehyde for 30 min and then in PBS for 2 h. Cornea, lens and retinal neurosensory layers were removed under a microscope. In the remaining RPE-choroid-sclera complex, 6-8 radial incision was made and the complex was flattened. The flats were placed in 1% Triton X-100 at room temperature for 2 h, followed by incubation with rhodamine-labeled castor bean lectin (1: 1000) at room temperature for 24 h. Finally, the flats were washed in tris-buffered saline (TBS) for 24 h. The flats were placed on slides, mounted with aqueous mounting medium and observed and photographed with a laser scanning confocal microscope.

ELISA Assay to Detect Vitreous EETs

ELISA assays were conducted by using an ELI-SA kit to detect the expression levels of vitreous EETs in rats. The ELISA kit was provided by Nanjing Jiancheng Company (Nanjing, China).

Immunohistochemical Staining

Paraffin sections were dewaxed by conventional methods. Sections containing CNV were selected for immunohistochemical staining. After soaking in 0.01 M PBS for 5 min, citrate buffer (pH = 6.0) were used for antigen retrieval with microwave heating for 10 min. Slides were washed with tap water and then with PBS for 3 times, 3 min each. After that, slides were incubated at room temperature for 30 min with $3\%~H_2O_2$ to eliminate the influence of endogenous peroxidase. After 3 washes

with PBS for 3 min each, slides were incubated with 5% normal goat serum diluted with PBS solution + 5% bovine serum albumin (BSA) at room temperature for 30 min. Afterward, the liquid was discarded and slides were not washed. The working concentration of the primary antibody was 1: 100. Incubation with primary antibody was conducted at 4°C for 24 h followed by 3 PBS washed for 3 min each. A secondary antibody was goat anti-rabbit or mouse IgG. Incubation was conducted at 37°C for 30 min followed by 3 PBS washed for 3 min each. Then, slides were placed in horseradish peroxidase enzyme working solution at 37°C for 30 min followed by 3 phosphate buffered saline with Tween 20 (PBST) washed for 3 min each. Color development was done with 3-amino-9-ethylcarbazole (AEC) chromogenic reagent for 5-10 min followed by Mayer's hematoxylin for 5-10 min. Slides were washed under running water and mounted with glycerol vinyl alcohol (GVA). They were observed under an optical microscope and photographed with a Charge-Coupled Device (CCD) camera.

Western Blotting

Rats were overdosed anesthetized and infused with saline solution. Eveballs were removed and the retina-RPE-choroid-sclera complexes were dissected out. Two retina-RPE-choroid-sclera complexes were combined to be one sample. Cell lysis buffer was added to lyse cells on ice. The supernatant was obtained by centrifugation. Protein was quantified by the bicinchoninic acid (BCA) method. Proteins were mixed with 5× loading buffer and boiled for 5 min. 40 mg total protein from each sample was loaded on a polyacrylamide gel containing a 12% separation gel and a 5% stacking gel. Gel was run under an 80 V constant voltage until the bromophenol blue migrates to the junction of the stacking gel and separating gel, then a constant 100 V voltage was applied until the bromophenol blue migrate to the bottom. Proteins on the gel were transferred to nitrocellulose membrane by electroporation (100 V, 90 min). The nitrocellulose membrane was blocked with 5% skim milk powder solution at 37°C for 1 h, and incubated with primary antibody (working concentration for both COX-2 and VEGF was 1: 200) at 4°C for overnight. Then, the membrane was incubated with horseradish peroxidase-conjugated secondary antibody (1: 20000) at room temperature for 1 h, and developed by ECL chromogenic system (Amersham, Buckinghamshire, UK). Images were scanned for analysis. β-actin was used as an internal reference. Gray values were analyzed by Kodardigtalscience1D data analysis software. The relative amounts of COX-2 and VGEF were recorded as the gray value ratios of COX-2 or VGEF to the corresponding β -actin¹³.

RT-PCR

After rats were given overdose anesthesia, eyeballs were immediately removed and the retina-RPE-choroid-sclera complexes were quickly dissected out. Two retina-RPE-choroid-sclera complexes were used as a sample. Total RNA was obtained by one-step extraction, and OD values were measured to determine total RNA concentrations. All OD values were between 1.8 to 2.0. cDNA was synthesized with 2 µg total RNA by using reverse transcription kits (Fermentas, Glen Brunie, MD, USA) according to the manufacturer's instructions. PCR amplifications were done with the synthesized cDNA as templates. Upstream and downstream primers for COX-2 were 5'-ACACTCTATCACTGGCATCC-3' 5'-GAAGGGACACCCTTTCACAT-3'. Primers for 561bp VEGF were 5'-AGCCCAT-GAAGTGGTGAA-3' and 5'-TGCGGATCT-TGGACAAAC-3'. Primers for 383 bp β-actin were 5'-CACCCGCGAGTACAACCTTC-3' and 5'-CCCATACCCACCATCACACC-3'. 207 bp (35). 5 µl of PCR products were separated on a 1.2% agarose gel followed by ethidium bromide staining to identify the RT-PCR products. Gel images were taken by Innotech gel imaging system (Alpha Innotech, NY, USA). Kodardigtalscience1D data analysis software was used to measure the optical densities. Relative expression of COX-2 and VEGF were recorded as the optical density ratios of COX-2 and VEGF to the corresponding β -actin. The red fluorescence area was measured with Image-proplus 6.0 (Version X; Media Cybernetics, Silver Springs, MD, USA).

Statistical Analysis

SPSS12.0 software (IBM, Armonk, NY, USA) was used to perform AVONA and SNK-q tests. *t*-tests for independent samples. *p*-value <0.05 was regarded as being statistically significant.

Results

Fluorescein Angiography

Retinal vessels of BN rats show radiating lines. After retinal laser photocoagulation, bubbles were observed in the central spots of photocoagulation. The photocoagulation spots

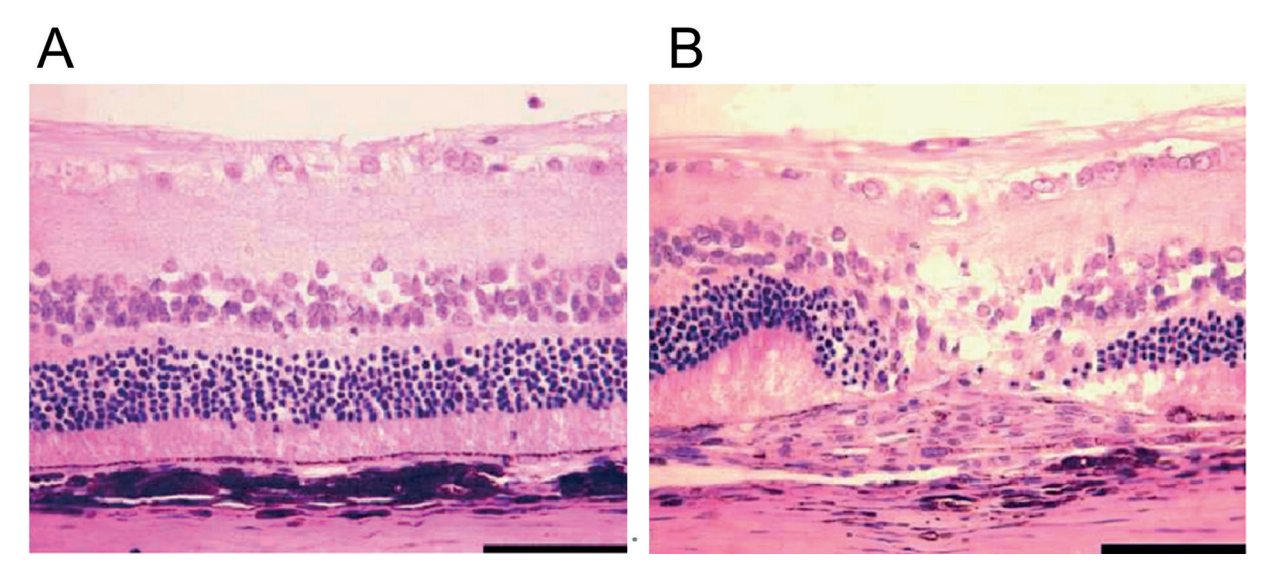


Figure 1. 200x inverted microscope HE staining. **A,** Retina and choroid of normal BN rats eyes. **B,** Spindle-shaped CNV formed under retina 14 days after photocoagulation. (bar = $100 \mu m$).

appeared to be thick white surrounded by a gray edema peripheral ring. Occasionally retinal or sub-retinal bleeding occurred. FFA examination of normal BN rats showed filling and radial retinal vascular. Choroid was filling and fused into the background fluorescence. The vascular wall was intact with no leakage. 7 days after photocoagulation, FFA results indicated small-sized disc-shaped fluorescein leakage in the photocoagulation area. Fluorescein leakage increased significantly 14 days after photocoagulation 14 d.

Pathological Staining

Normal rats showed clear and complete retina and choroid. 14 days after photocoagulation, CNV was produced, containing neutrophils, pigmented macrophages, fibroblasts, collagen fibers, neovascularization surrounded by proliferating and migrating RPE cells (Figure 1). CNV thickness was significantly reduced (p<0.01, Figure 2) in the treatment group (45.68 ± 6.37 µm, n = 11) compared with the control group (69.82 ± 7.31 µm, n = 13) on day 14 after photocoagulation, suggesting that

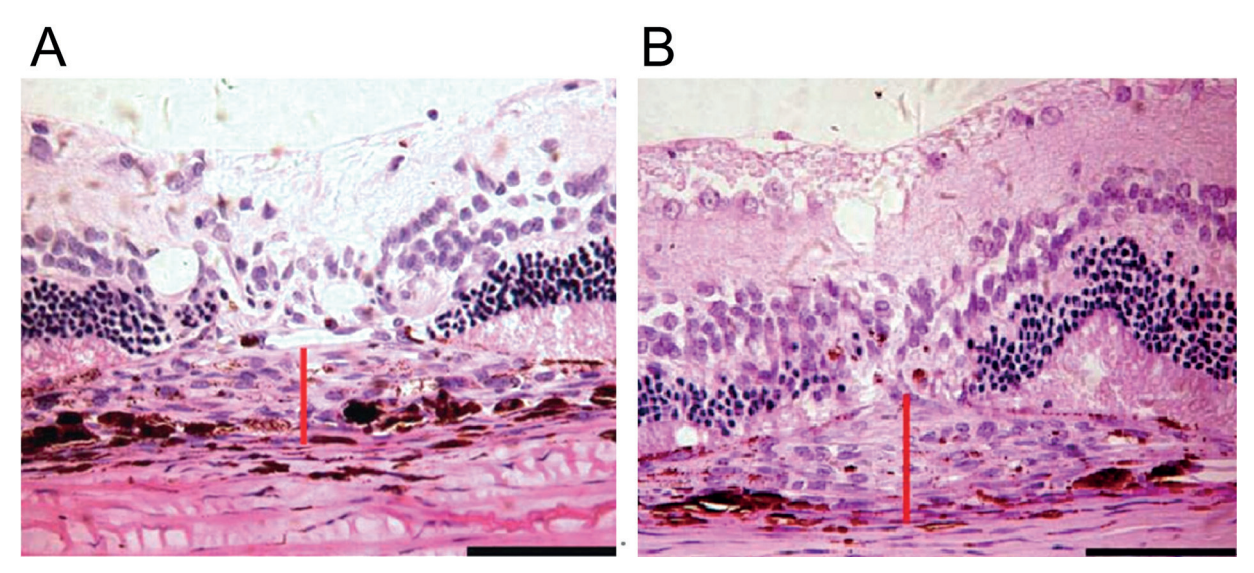


Figure 2. 200x inverted microscope HE staining. A, Celecoxib treatment group. B, Control group. (bar = 100 μm).

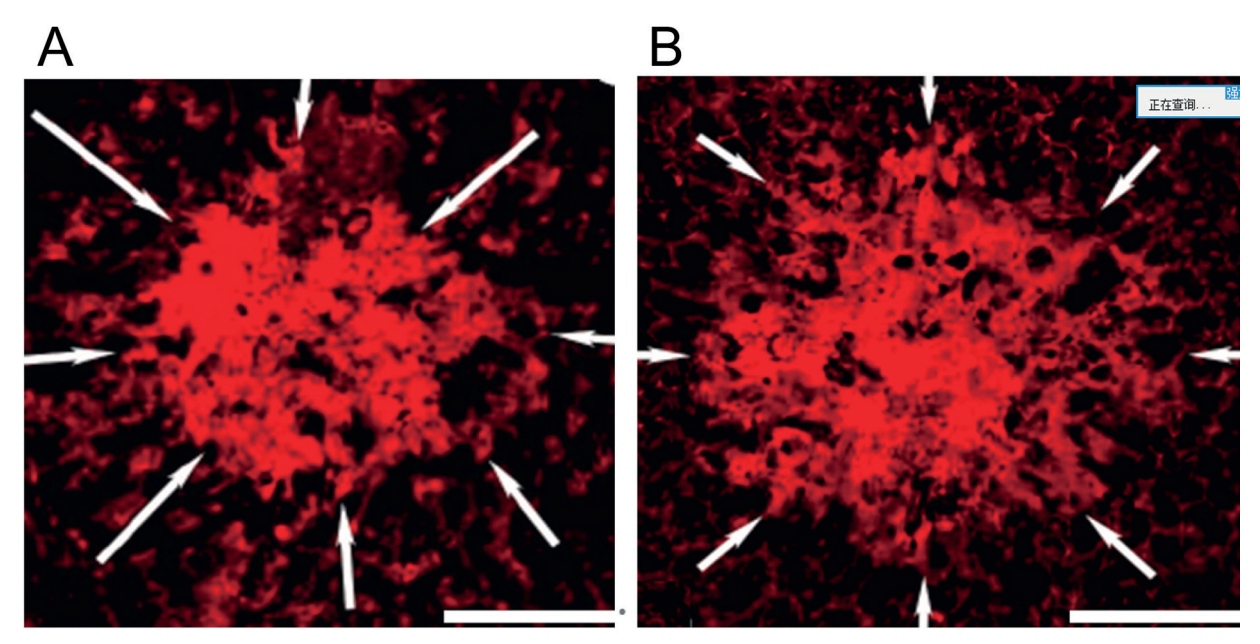


Figure 3. RPE- choroid - sclera flat mounts. *A*, Treatment group. *B*, Control group. (20x).

intravitreal injection of selective COX-2 inhibitor celecoxib (1 mg/ml) can inhibit CNV thickness.

RPE-Choroid-Sclera Flat Mounts

14 days after photocoagulation, CNV area was significantly reduced (p<0.01) in the treatment group (60830 \pm 6719 pixels 2n = 13) compared with the control group CNV area (85965 \pm 7457 pixels 2 n = 11), suggesting that intravitreal injections of selective COX-2 inhibitor celecoxib (1 mg/ml) significantly inhibited CNV area. See Figure 3.

Immunohistochemistry

COX-2 was expressed in the inner nuclear layer and inner and outer plexiform layer of normal rats. 7 days after photocoagulation, besides expression in the above tissue, COX-2 was also detected in vascular endothelial cells and stromal cells in the CNV area, mainly in the cytoplasm. VEGF was seen in the retinal ganglion cell layer, inner nuclear layer and RPE cell layer of normal rats. 7 days after photocoagulation, besides expression in the above tissues, the expression of VEGF was detected in vascular endothelial cells, stromal cells and pigmented macrophages in the CNV area (Figure 4).

Western Blotting Results

Expression of COX-2 in normal rat retina-R-PE-choroid-sclera complexes was low. Its expression was upregulated 1 day after photocoagula-

tion, peaked at 3 days after photocoagulation, and decreased afterward. Weak expression was still detected 14 days after photocoagulation (Figure 5A). Semi-quantitative analysis showed that 3 days after photocoagulation, COX-2 expression was significantly higher than any other time point (p<0.01, Figure 5B). VEGF in the normal rat retina-RPE-choroid-sclera complexes expressed at a low-level. VEGF was upregulated 1 day after photocoagulation. Its expression peaked at 7 days after photocoagulation and then decreased with weak expression still detected on day 14 after photocoagulation. Semi-quantitative analysis indicated expression of VEGF on day 1, 3, and 7 after photocoagulation was higher (p<0.01) than before and 14-day after photocoagulation. Expression of VEGF had no significant differences among groups of 1-day, 3-day and 7-day after photocoagulation (p>0.05, Figure 5C). These results indicated that during the formation of CNV, COX-2 protein expresses earlier than VEGF protein; intravitreal injection of selective COX-2 inhibitor celecoxib (1 mg/ml) can inhibit VEGF expression.

VEGF Expression Levels After Intravitreal Injection of Selective COX-2 Inhibitor

VEGF expression was examined 48 h after intravitreal injection of COX-2 inhibitor celecoxib. The results showed that VEFG expression level was statistically lower (p<0.05) in the treatment group than in the control group (Figure 6).

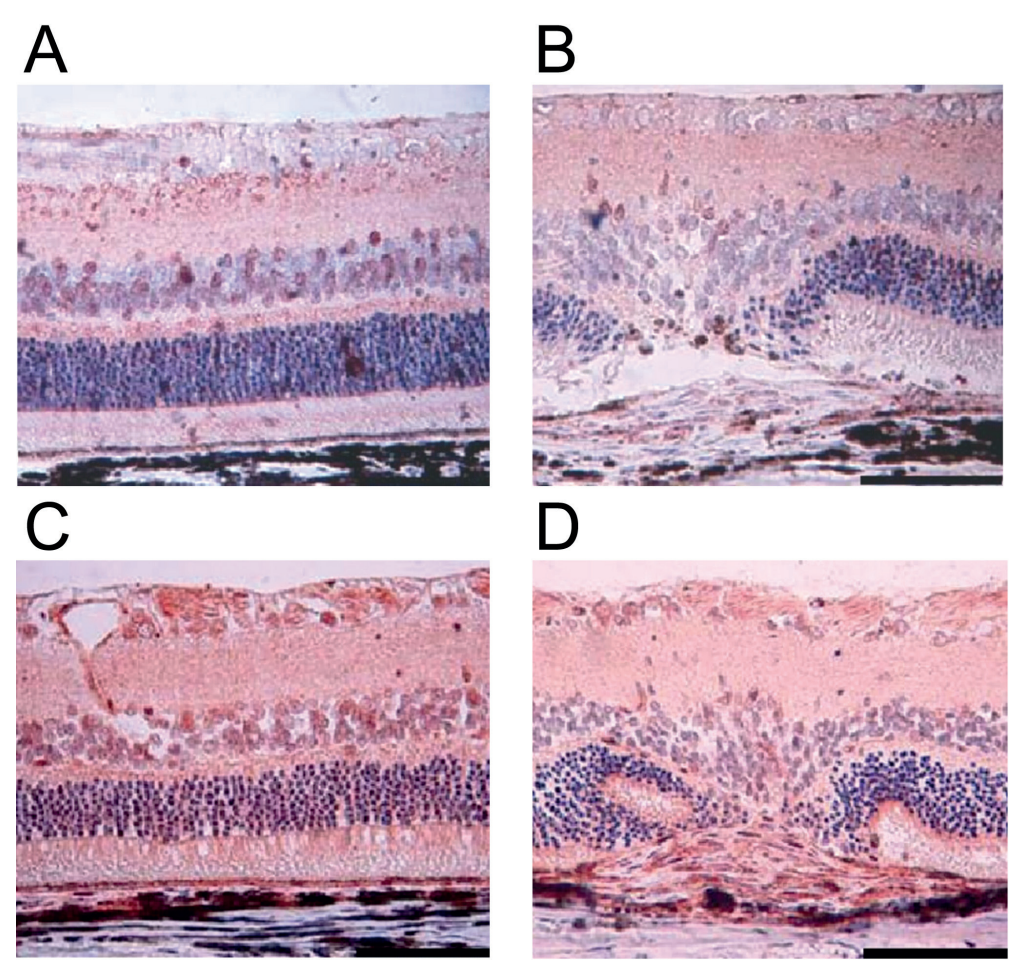


Figure 4. Immunohistochemistry results of COX-2. A, COX-2 expression in normal retina. B, Expression of COX-2 in the photocoagulation area 7 days after photocoagulation. C, VEGF expression in normal retina. D, Expression of VEGF in the photocoagulation area 7 days after photocoagulation. (AEC bar = $100 \mu m$).

OR-PCR Results

COX-2 mRNA exhibited low-level expression in the retina-RPE-choroid-sclera complexes of normal rats; its expression was upregulated 1 day after photocoagulation, peaked at 3 days after and then decreased. A weak expression was still found on 14 days after photocoagulation. Semi-quantitative analysis showed significantly higher expression (p<0.05) on day 3 after photocoagulation than other time points. VEGF mRNA level was low in retina-choroid-sclera complexes of normal rats. VEGF level increased 1 day after photocoagulation and peaked on 7 days after. Its weak expression was still detected 14 days after photocoagulation. Semi-quantitative analysis indicated that VEGF expression levels were significantly higher (p<0.05) on 3-day and 7-day after photocoagulation than the other time points, but there was no significant difference (p>0.05) between the 3-day and the 7-day groups (Figure 7). These results suggest that during the process of CNV generation, COX-2 mRNA expression was earlier than that of VEGF. The results also showed that intravitreal injection of selective COX-2 inhibitors celecoxib (1 mg/ml) could inhibit VEGF mRNA expression (p<0.05), but not COX-2mRNA (p>0.05) (Figure 7).

ELISA Results of Rat Vitreous EETs

Enzyme-linked immunosorbent assay was used to detect vitreous EETs levels in each group of rats. It was found that vitreous EETs expression levels in rats in the celecoxib treatment group significantly increased (p<0.05) compared with the control group (Table I).

Discussion

Age-related macular degeneration (AMD) usually refers to the central macular lesions¹².

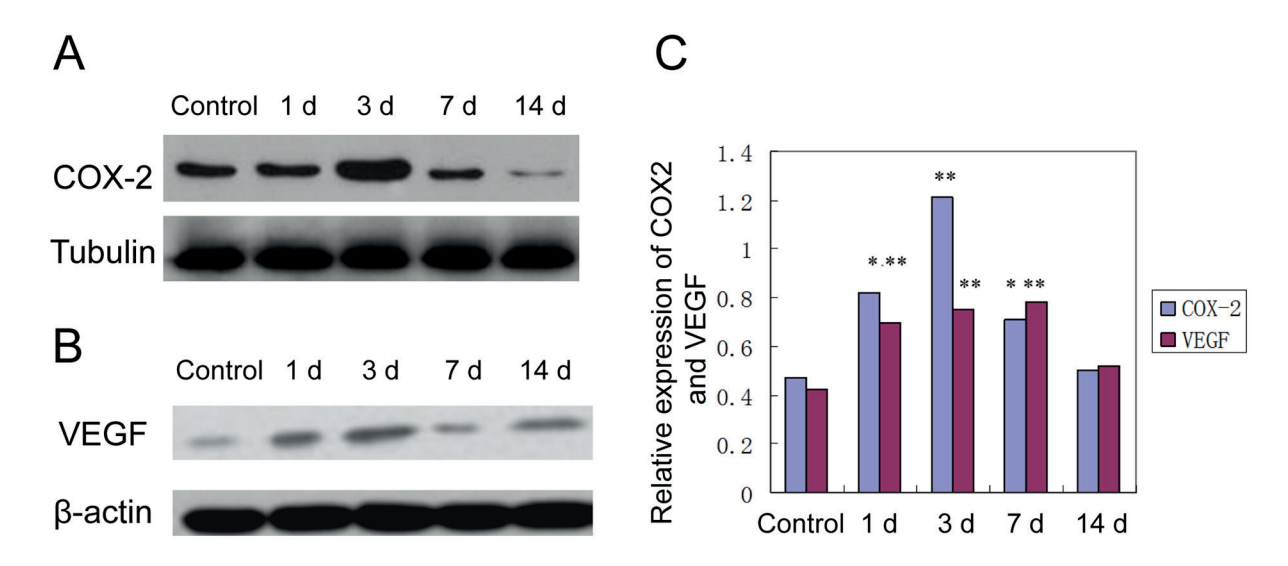


Figure 5. COX-2 had low-expression in normal rat retina-RPE-choroid-sclera complexes. A, Its expression was upregulated 1 day after photocoagulation. Peak expression was observed on day 3 after photocoagulation. Its expression decreased afterward and weak expression was still found on day 14 after photocoagulation; semi-quantitative analysis indicated that COX-2 expression was significantly higher on day 3 after photocoagulation than the rest of the time points (p<0.01); B, VEGF had low expression in normal rat retina-RPE-choroid-sclera complexes. Its expression was upregulated 1 day after photocoagulation. Peak expression was detected on day 7 after photocoagulation and then decreased. Weak expression was still found 14 days after photocoagulation; C, Semi-quantitative analysis: VEGF expression on day 1, 3 and 7 after photocoagulation was significantly higher (p<0.01) than before and 14 days after photocoagulation, with no significant differences among the day 1, 3 and 7 groups (p>0.05). These results indicated that during the generation of CNV, COX-2 protein expresses earlier than VEGF protein.

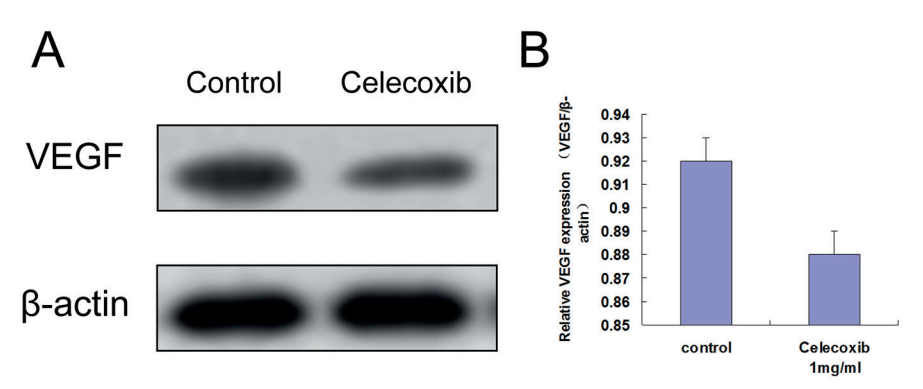


Figure 6. VEGF expression detected by Western blot. **A,** VEGF expression after intravitreal injection COX-2 inhibitor celecoxib. **B,** VEGF expression level was significantly lower (p<0.05) in the treatment group compared with the control group.

This area of the retina plays critical roles in fine vision, image resolution, and outside light stimuli capture¹³. There are some major identifiable structures in human macula. The retina contains an inner retinal neuro-epithelium layer, photoreceptor cell layer and the bottom layer of retinal pigment epithelium (RPE)¹⁴. The bruch membrane (BM) separated choroid and choroidal capillaries (CC), and the base layer is formed. The retina also contains two types of photoreceptor cells, the rods and cones. Typically, the number of rod cells

significantly excesses that of cones, and there are as many as 120 million rod cells. Rod cells are

Table I. ELISA results of rat vitreous EETs levels (ng / ml).

Group	EETs (ng/ml)
Control Treatment	182.3±31.8 402.4±10.9
<i>t</i> -value <i>p</i> -value	11.28 0.02

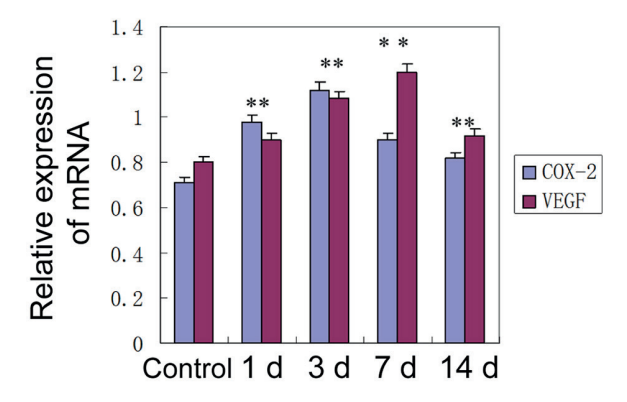


Figure 7. mRNA expression of VEGF and COX-2 at different time-points was detected by RT-PCR.

more light-sensitive than cone cells and are important for visual function under low light conditions (dark vision)¹⁵⁻¹⁷. But rod cells are not sensitive to colors and have low spatial acuity. In contrast, the number of cone cell usually varies between 0.6 to 7 million. Under good light conditions¹⁸, cone cells are more active and play a major role in vision, also known as light vision. They have color differentiation ability and contribute to high-level spatial resolution¹⁹. Under certain circumstances, such as aging and laser irradiation, normal retina tissues can easily be disrupted, choroidal neovascularization will be stimulated to induce macular degeneration. CNV formation is a very complex process, affected by many factors and undergoes fine regulation¹². De Jong¹⁴ observed that COX-2 expression was detected in resected human CNVs, and its expression was positively correlated with age. As a selective COX-2 inhibitors, celecoxib has displayed good therapeutic effects in the treatment and relief of adult rheumatoid arthritis symptoms. Previous *in vitro* experiments have shown that celecoxib selectively inhibits COX-2. The inhibiting effect was about 155~300 times stronger than for COX-1²⁰. The results suggested the possibility of using celecoxib to treat corneal neovascularization, diabetic retinopathy and other diseases²²⁻²³, but whether celecoxib can be used on CNV is currently still controversial. The bioavailability of celecoxib was 54 times more in animals receiving subconjunctival injection than in those receiving an intraperitoneal injection, which led them to propose that celecoxib mainly functions by infiltration around the drug injection sites²⁴. Another recent discovery showed that compared with SD rats, BN rats had more celecoxib in pigmented RPE-choroid but less celecoxib in the retina and vitreous, no matter whether they received periocular injection or periocular administration of sustained release particles²⁵.

Selective COX-2 inhibitors can suppress normal biological activities of EETs in vivo. In its presence, the CNV lesion area might have other angiogenic factors to promote VEGF expression. For example, COX-2 inhibitors could inhibit VEGF produced by the monocyte/macrophage migration, but could not suppress VEGF upregulation by RPE cells in a COX-independent way, but the exact mechanism remains unclear²⁵. Previous studies usually only measured CNV sizes by RPE- choroid-sclera flat mounts, but did not employ FFA and histopathological methods. Therefore, evaluation of CNV and its effect on VEGF expression was not clear. In our study, the CNV model in BN rats was induced by a 532 nm laser photocoagulation. Our FFA and HE staining results indicated that 14 days after photocoagulation, CNV was successfully induced. For the first time, our study demonstrated that intravitreal injection of the selective COX-2 inhibitor celecoxib immediately following laser photocoagulation could significantly inhibit the thickness and area of CNV. At the same time, this treatment could effectively improve the level of intravitreal EETs expression. However, to determine the underlying mechanism and any indications for therapeutic treatment of human CNV-related diseases, will require more research.

Conclusions

532 nm laser photocoagulation is a fast and efficient way to create CNV BN rat models with high success. Intravitreal injection of celecoxib can suppress laser-induced macular degeneration, CNV thickness and improve vitreous EETs levels. The COX-2 expression is upregulated in the early phase of laser-induced CNV, which may play an important role in regulating VEGF expression.

Conflict of interest

The authors declare no conflicts of interest.

References

 LADAS DS, KOUTSANDREA C, KOTSOLIS AI, GEORGALAS I, Moschos MM, Ladas ID. Intravitreal ranibizumab for choroidal neovascularization secondary to angiod streaks. Comparison of the 12 and

- 24-month results of treatment in treatment-naïve eyes. Eur Rev Med Pharmacol Sci 2016; 20: 2779-2785.
- Dubois RN, Abramson SB, Crofford L, Gupta RA, Simon LS, Van De Putte LB, Lipsky PE. Cyclooxygenase in biology and disease. Faseb J 1998; 12: 1063-1073.
- GASS JD. Biomicroscopic and histopathologic considerations regarding the feasibility of surgical excision of subfoveal neovascular membranes. Trans Am Ophthalmol Soc 1994; 92: 91-111.
- 4) GROSSNIKLAUS HE, GREEN WR. Choroidal neovascularization. Am J Ophthalmol 2004; 137: 496-503.
- BHUTTO IA, McLEOD DS, HASEGAWA T, KIM SY, MERGES C, TONG P, LUTTY GA. Pigment epithelium-derived factor (PEDF) and vascular endothelial growth factor (VEGF) in aged human choroid and eyes with age-related macular degeneration. Exp Eye Res 2006; 82: 99-110.
- LAU LI, CHEN SJ, CHENG CY, YEN MY, LEE FL, LIN MW, HSU WM, WEI YH. Association of the Y402H polymorphism in complement factor H gene and neovascular age-related macular degeneration in Chinese patients. Invest Ophthalmol Vis Sci 2006; 47: 3242-3246.
- KIM NR, KANG JH, KWON OW, LEE SJ, OH JH, CHIN HS. Association between complement factor H gene polymorphisms and neovascular age-related macular degeneration in Koreans. Invest Ophthalmol Vis Sci 2008; 49: 2071-2076.
- EL-ASRAR AM, MISSOTTEN L, GEBOES K. Expression of cyclo-oxygenase-2 and downstream enzymes in diabetic fibrovascular epiretinal membranes. Br J Ophthalmol 2008; 92: 1534-1539.
- Xu J, Wang Y, Li Y, Yang X, Zhang P, Hou H, Shi Y, Song C. Inhibitory efficacy of intravitreal dexamethasone acetate-loaded PLGA nanoparticles on choroidal neovascularization in a laser-induced rat model. J Ocul Pharmacol Ther 2007; 23: 527-540.
- 10) Lu H, Cui J, Dong H, Luo B, Xiu W, Li H. [Clinical observation of a new anti-VEGF drugs conbercept for wet age-related macular degeneration]. Zhonghua Yan Ke Za Zhi 2015; 51: 818-821.
- TAKAHASHI H, YANAGI Y, TAMAKI Y, UCHIDA S, MURANAKA K. COX-2-selective inhibitor, etodolac, suppresses choroidal neovascularization in a mice model. Biochem Biophys Res Commun 2004; 325: 461-466.
- 12) YANG XM, WANG YS, ZHANG J, LI Y, XU JF, ZHU J, ZHAO W, CHU DK, WIEDEMANN P. Role of PI3K/Akt and MEK/ERK in mediating hypoxia-induced expres-

- sion of HIF-1alpha and VEGF in laser-induced rat choroidal neovascularization. Invest Ophthalmol Vis Sci 2009; 50: 1873-1879.
- AMBATI J, AMBATI BK, YOO SH, IANCHULEV S, ADAMIS AP. Age-related macular degeneration: etiology, pathogenesis, and therapeutic strategies. Surv Ophthalmol 2003; 48: 257-293.
- 14) DE JONG PT. Age-related macular degeneration. N Engl J Med 2006; 355: 1474-1485.
- 15) McGimpsey SJ, Chakravarthy U. VEGF-targeted therapy and beyond: pharmacotherapy and emerging treatments in age-related macular degeneration. Expert Rev Clin Pharmacol 2010; 3: 243-252.
- PAULUS YM, SODHI A. Anti-angiogenic therapy for retinal disease. Handb Exp Pharmacol 2016. [Epub ahead of print]
- RESNIKOFF S, PASCOLINI D, ETYA'ALE D, KOCUR I, PARA-RAJASEGARAM R, POKHAREL GP, MARIOTTI SP. Global data on visual impairment in the year 2002. Bull World Health Organ 2004; 82: 844-851.
- 18) CAMPOCHIARO PA. Retinal and choroidal neovascularization. J Cell Physiol 2000; 184: 301-310.
- 19) MALONEY SC, FERNANDES BF, CASTIGLIONE E, ANTECKA E, MARTINS C, MARSHALL JC, DI CESARE S, LOGAN P, BURNIER MJ. Expression of cyclooxygenase-2 in choroidal neovascular membranes from age-related macular degeneration patients. Retina 2009; 29: 176-180.
- 20) SIMMONS DL, BOTTING RM, HLA T. Cyclooxygenase isozymes: the biology of prostaglandin synthesis and inhibition. Pharmacol Rev 2004; 56: 387-437.
- PAKNESHAN P, BIRSNER AE, ADINI I, BECKER CM, D'AMATO RJ. Differential suppression of vascular permeability and corneal angiogenesis by nonsteroidal anti-inflammatory drugs. Invest Ophthalmol Vis Sci 2008; 49: 3909-3913.
- 22) EL-ASRAR AM, MISSOTTEN L, GEBOES K. Expression of cyclo-oxygenase-2 and downstream enzymes in diabetic fibrovascular epiretinal membranes. Br J Ophthalmol 2008; 92: 1534-1539.
- AYALASOMAYAJULA SP, KOMPELLA UB. Retinal delivery of celecoxib is several-fold higher following subconjunctival administration compared to systemic administration. Pharm Res 2004; 21: 1797-1804.
- 24) CHERUVU NP, AMRITE AC, KOMPELIA UB. Effect of eye pigmentation on transscleral drug delivery. Invest Ophthalmol Vis Sci 2008; 49: 333-341.
- CASTRO MR, LUTZ D, EDELMAN JL. Effect of COX inhibitors on VEGF-induced retinal vascular leakage and experimental corneal and choroidal neovascularization. Exp Eye Res 2004; 79: 275-285.